



ANNUAL REVIEWS **Further**

Click [here](#) to view this article's online features:

- Download figures as PPT slides
- Navigate linked references
- Download citations
- Explore related articles
- Search keywords

Molecular Plasmonics

Andrew J. Wilson and Katherine A. Willets

Department of Chemistry, Temple University, Philadelphia, Pennsylvania 19122;
email: kwillets@temple.edu

Annu. Rev. Anal. Chem. 2016. 9:27–43

First published online as a Review in Advance on
March 30, 2016

The *Annual Review of Analytical Chemistry* is online
at anchem.annualreviews.org

This article's doi:
10.1146/annurev-anchem-071015-041612

Copyright © 2016 by Annual Reviews.
All rights reserved

Keywords

active plasmonics, plasmon-molecule coupling, polycyclic aromatic hydrocarbons, SERS, surface plasmon resonance

Abstract

In this review, we survey recent advances in the field of molecular plasmonics beyond the traditional sensing modality. Molecular plasmonics is explored in the context of the complex interaction between plasmon resonances and molecules and the ability of molecules to support plasmons self-consistently. First, spectroscopic changes induced by the interaction between molecular and plasmonic resonances are discussed, followed by examples of how tuning molecular properties leads to active molecular plasmonic systems. Next, the role of the position and polarizability of a molecular adsorbate on surface-enhanced Raman scattering signals is examined experimentally and theoretically. Finally, we introduce recent research focused on using molecules as plasmonic materials. Each of these examples is intended to highlight the role of molecules as integral components in coupled molecule-plasmon systems, as well as to show the diversity of applications in molecular plasmonics.

SPR: surface plasmon resonance

LSPR: localized surface plasmon resonance

SERS: surface-enhanced Raman scattering

INTRODUCTION

In writing a review on molecular plasmonics, one is first faced with the challenge of defining the term, given the many usages in the literature. For example, molecular plasmonics has been invoked to describe how plasmonic materials can interact with nearby molecules by enhancing their spectroscopic signatures, thus allowing for plasmon-enhanced sensing and detection (1–3). Alternatively, molecular plasmonics is used to describe how plasmonic materials behave in an analogous fashion to molecules, such as in the plasmon hybridization model, which treats the energy of coupled plasmon modes in a dimer of nanoparticles in a similar fashion to the bonding and antibonding orbitals in a diatomic molecule, such as H_2 (4–6). In other usages, molecular plasmonics describes an active interaction between a molecule and a plasmonic material in which a change in one of the materials induces a spectroscopic change in the other (7–10). More recently, the term has been used in a very literal sense to describe how certain highly conjugated molecular species can support plasmons (11). Given the vast array of experiments to which the term molecular plasmonics has been linked, writing a review on this topic is a large task because it requires either picking a favored definition and ignoring other contributions to the field or summarizing a series of experiments that fall into the broader context of the term. In this review, we have chosen the latter approach, selecting various examples that highlight both active interactions between molecules and plasmonic materials and cases in which the molecule and the plasmonic material are one and the same.

To begin, we first need to define a plasmon. A plasmon is the light-driven collective oscillation of the surface conduction electrons in materials with a negative real and small positive imaginary dielectric constant (12). The electric field component of light drives a collective displacement of electrons within a material, leading to either a propagating electron density wave (a plasmon polariton) or a standing wave (a localized surface plasmon). The former is typically associated with either thin films or quasi-one-dimensional structures (such as a nanowire with a subwavelength diameter and a micron-sized length), which allow the wave to be confined along the nanoscale dimension of the material while propagating along the extended dimension(s). Momentum matching requires that the excitation light have the correct angle of incidence and resonance wavelength, the surface plasmon resonance (SPR), to excite a plasmon in these higher-dimension materials. On the other hand, localized surface plasmons are excited in nanoparticles in which the dimensions are smaller than the wavelength of light, leading the plasmon to be localized at the nanostructure surface (12). In the case of nanoparticles, the localized surface plasmon resonance (LSPR) defines the color of the nanoparticle and depends strongly on the shape, size, local environment, and composition of the nanostructure (13, 14). Although plasmons have historically been associated with noble metals, such as silver and gold, new plasmonic materials such as metal oxides and graphene have recently emerged, expanding plasmonics into new wavelength regimes and new potential applications (15, 16).

In analytical chemistry, the interaction between plasmonic materials and molecules has focused primarily on sensing applications. For example, the sensitivity of the (L)SPR to the local environment has led to the development of plasmon-based refractive index sensors (17, 18). In this case, the plasmonic material is often functionalized with a capture ligand, such as an antibody, which then binds a target molecule of interest, changing the local refractive index at the nanoparticle surface and leading to a measurable shift in the plasmon resonance (19). As an alternative sensing strategy, surface-enhanced spectroscopies, notably surface-enhanced Raman scattering (SERS), benefit from local electromagnetic field enhancements that arise at nanostructure surfaces upon plasmon excitation (20). Here, a molecule on or near the surface experiences enhancement of both the excitation field as well as its Raman scattered light, leading to enhancements of spectroscopic

signals that can exceed 10^8 (21). In many of the theoretical descriptions of SERS, the molecule is treated as a passive beneficiary of the locally enhanced electromagnetic fields at the nanoparticle surface, such that only the plasmonic properties of the nanostructure dictate the magnitude of the SERS enhancement. However, as discussed further below, recent experimental and theoretical work has shown that the molecule plays an active role in defining how plasmon excitation and emission impact signal enhancement, suggesting a more intimate relationship between the plasmonic material and the molecule.

In this review, we address recent advances in molecular plasmonics that move beyond the traditional sensing paradigm and probe more deeply into the relationship between molecules and plasmons. First, we discuss experiments in which coupling between molecular and plasmon resonances induce a spectral change in the LSPR spectrum of metallic nanostructures. Next, we extend this concept into the realm of active molecular plasmonics, in which the properties of a plasmonic material are actively and reversibly controlled by changing the state of a nearby molecule. We then discuss recent advances in SERS that show how the presence of a molecule can perturb the local electromagnetic field, leading to new theoretical descriptions of SERS enhancements that account for both the polarizability of the molecule and the plasmonic substrate. Finally, we discuss the emerging field of molecule-based plasmonics, in which doped, highly conjugated molecules are able to support localized surface plasmons. In each of these experiments, we highlight the role that the (oft-ignored) molecule plays in dictating the plasmonic response of the highly coupled system.

SPECTRAL SIGNATURES OF PLASMON-MOLECULE COUPLING

Most refractive index (L)SPR sensing experiments are based on detecting molecules with electronic resonances far from the plasmon resonance of the substrate, leading to a straightforward linear relationship between the plasmon resonance peak shift and the magnitude of the refractive index change induced upon analyte binding (12). However, in 2006, Haes et al. (22) showed that a molecule with an electronic resonance that overlapped with the plasmon resonance of a nanoparticle substrate could generate a significantly different plasmon resonance shift response. **Figure 1** shows an example in which the change in the LSPR of a silver nanoprism array on glass was measured upon adsorption of a magnesium (II) porphyrine (MgPz) derivative (**Figure 1a**). When the plasmon resonance of the array was blue-shifted of the molecular resonance (**Figure 1a**), very little shift in the LSPR was observed upon adsorption of the MgPz, although the plasmon resonance spectrum was damped (**Figure 1d**). On the other hand, a relatively large shift in the LSPR (~ 60 nm) was observed when the plasmon resonance was red-shifted of the molecular resonance (**Figure 1b**). Farther from the molecular resonance, the LSPR shifts the expected amount (~ 20 nm) based on the refractive index change induced by the adsorbed molecule (**Figure 1c**). The authors noted that although the LSPR-dependent shift response shown in **Figure 1a** qualitatively follows the real component of the refractive index, as predicted by the Kramers–Kronig transformation of the absorption spectrum, the magnitudes of the LSPR shifts are not correctly predicted by this relationship. To reconcile this discrepancy, the authors used discrete dipole approximation calculations to show that the origin of this effect could be due to the wavelength-dependent polarizability of the adsorbed molecules either constructively or destructively interfering with the plasmon modes of the nanostructures, leading to either enhanced or suppressed plasmonic shifts, respectively.

Beyond influencing the shift in the plasmon resonance induced by molecular adsorbates, overlapping plasmonic and electronic resonances can also lead to pronounced dips or splitting in the plasmon resonance spectrum. Kometani et al. (23) reported this effect for nanostructures coated with J-aggregates of cyanine dyes. In their experiment, large dips in the plasmon resonance spectra

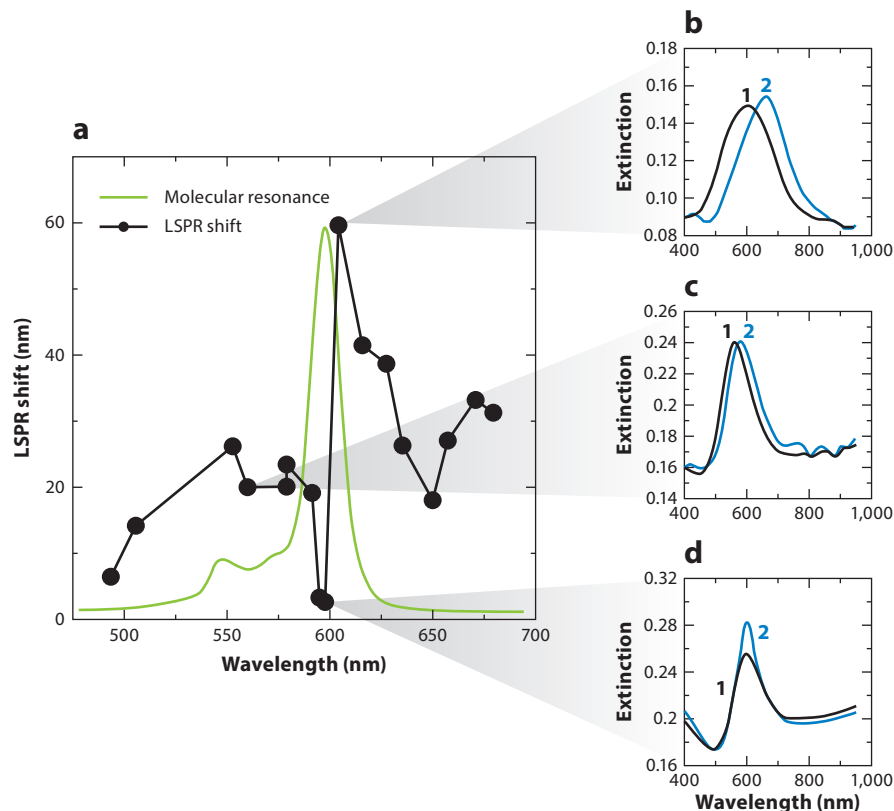


Figure 1

(a) Localized surface plasmon resonance (LSPR) shift as a function of peak plasmon wavelength upon adsorption of magnesium (II) porphyrazine (MgPz) on silver nanoprism arrays with varying plasmon resonances. The green curve shows the molecular absorbance spectrum of MgPz. (b–d) LSPR spectra before (black curve, 1) and after (blue curve, 2) adsorption of MgPz when the plasmon resonance of the array is (b) slightly red-shifted, (c) off resonance, and (d) slightly blue-shifted of the MgPz electronic resonance. Reprinted with permission from Reference 22. Copyright 2006 American Chemical Society.

of gold nanoparticles were measured upon adsorption of the J-aggregates from solution, whereas silver nanoparticles showed the appearance of a new peak when the J-aggregates were introduced. Wiederrecht et al. (24) suggested that the origin of the different spectral features depends on how the J-aggregate excitons couple to the electrons within the nanostructure: Silver shows a new peak due to constructive interference between the exciton mode and the unbound conduction electrons that make up the plasmon, whereas gold shows a dip in the LSPR spectrum due to coupling between the exciton and bound electrons within the gold. Within this model, the coupled plasmon-exciton system leads to a new hybrid state, a plexciton, as further shown by experiments from Halas and coworkers (25) on J-aggregate functionalized gold nanoshells. However, more recent work from Shegai and coworkers (26) studied silver nanoprisms on J-aggregate sheets and found distinct plasmon splitting behaviors, which they explained using a Rabi splitting framework in which the plasmonic nanoparticle behaved as an optical cavity. Thus, despite the clear evidence for an interaction between the molecular and plasmonic resonances in this coupled system, the best way to describe the interaction—for example, a dip, a splitting, a new state, or some hybrid—is still somewhat under debate.

Adding to the picture of different plasmon-molecule coupling behaviors, Lee and coworkers (27) observed dips in the plasmon resonance spectrum of gold nanoparticles with cytochrome *c* adsorbed to the surface. The dips appeared at the same frequency as the absorption bands of the cytochrome *c*, and by toggling the molecule between its oxidized and reduced forms, they could move the frequencies at which the dips appeared, thus verifying that the cytochrome *c* was responsible for the observed effects. They named the new phenomenon plasmon resonance energy transfer, implying that an energy transfer mechanism was responsible for the observed dips in the LSPR spectra.

To reconcile these different observations, Lin and coworkers (28) proposed a model to explain how plasmon-molecule coupling could move from the splitting regime to the energy transfer regime, simply by tuning the oscillator strength and line width of the molecular transition, in addition to the thickness of the molecular shell. When the line width of the electronic resonance is narrow, increasing the oscillator strength of the molecular adsorbate leads to plasmon splitting, which is characterized by broadening of the plasmon resonance, accompanied by the emergence of a small shoulder. With a broader molecular resonance line width, the plasmon resonance spectrum shows a strong dip, consistent with an energy transfer mechanism. However, if the molecular transition becomes too broad, the plasmon resonance can ultimately be quenched, leading to a loss in the extinction. Thus, these calculations indicate how it is possible to tune the spectral signatures associated with the interaction between molecular and plasmon resonances, simply by changing the properties of the molecular adsorbate.

The lesson from the studies described above is that the plasmon resonance spectrum can be impacted by the presence of molecules on the surface in a variety of ways due to coupling between the electronic and plasmonic resonances. Not only does this coupling offer the opportunity to enhance the spectral sensitivity in LSPR sensing assays (29), but there is also significant potential for exploiting these properties for photonic and optoelectronic devices. In the next section, we describe how this phenomenon leads to active control over the plasmonic response of a system, simply by modulating the properties of the molecular species.

ACTIVE MOLECULAR PLASMONICS

Reversibly tuning the LSPR of a plasmonic system has typically been accomplished by changing the properties of the metallic nanoparticles themselves, leading to active plasmonics. For example, linked dimers of nanoparticles, known as plasmon rulers, show distance-dependent plasmon resonance spectra due to separation-dependent hybridization of the plasmon modes (30). By using linkers that can expand and contract, the LSPR spectrum can be reversibly modulated (31). Another approach is to pattern noble metal nanoparticles onto flexible substrates, where the pitch and nanoparticle separation can be tuned by applying a strain, leading to a predictable and reversible plasmonic response as the separation between the nanoparticles is changed (32–34). As an alternate strategy, the charge density of the nanoparticles can be changed by applying an electrochemical potential, as shown by Mulvaney and coworkers (35). In their work, electron injection into gold nanoparticles leads to a reversible blue shift in the plasmon resonance due to an increase in the charge density of an individual nanoparticle. However, the tunable bandwidth of this active plasmonic system is narrow (~ 10 nm) because the number of electrons electrochemically transferred is small compared to the free electron density in the metal. Alternatively, doped semiconductor nanoparticles have also been shown to support plasmon resonances that are tunable (36). These materials have a much lower electron density compared to a metal, which allows larger and more sensitive spectral tuning of the plasmon resonance under electrochemical control

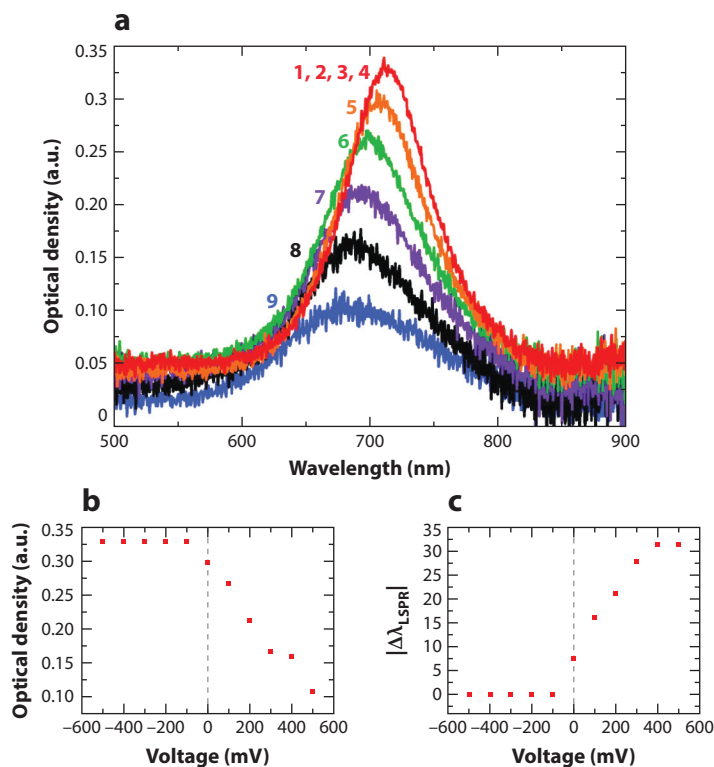


Figure 2

Example of an active molecular plasmonic device. (a) A polyaniline film is spin cast on an array of gold nanoparticles in an electrochemical cell, and the plasmon resonance spectrum is measured as a function of applied potential: (1–4) from -500 to -100 , (5) 0 , (6) $+100$, (7) $+200$, (8) $+300$, and (9) $+500$ mV versus Ag/AgCl. The molecular resonance of the polyaniline changes as the polymer is oxidized, resulting in a voltage-dependent (b) change in the plasmon intensity and (c) shift in the localized surface plasmon resonance. Reprinted with permission from Reference 39. Copyright 2008 American Chemical Society.

(37). As the development of new plasmonic materials continues, direct resonance tuning has the potential to become increasingly important for active devices.

On the other hand, the vastness of tunable molecular properties currently offers a broader range of strategies and spectral bandwidth for advances in active molecular plasmonics. By inducing a change in the electronic resonance of an adsorbed molecule, a change in the optical response of the coupled molecule-plasmon system can be realized. One simple strategy for changing the electronic resonance of a molecular adsorbate is through redox chemistry. For example, Leroux et al. (38) demonstrated one of the first active molecular plasmonic devices by electrochemically controlling the reduction and oxidation of an electrochromic polymer, polyaniline, deposited on an array of gold nanoparticles. In this case, two effects are at play: a change in the local refractive index and a change in the electronic resonance upon polyaniline oxidation, leading to a blue shift and a damping in the LSPR spectrum, respectively. **Figure 2** shows an example in which a gold nanoparticle array displays a voltage-dependent shift in both the plasmon resonance and the optical density as the polyaniline is oxidized (39). The magnitude of the response can be tuned by changing the grating constant of the nanoparticle array (38), plasmon resonance of the array (40),

polarization of the excitation (in the case of anisotropic nanoparticles) (40), and thickness of the polyaniline film (41).

A second strategy for exploiting changes in the molecular resonance to control the plasmonic response of a hybrid molecule-plasmon system is to use a photochromic dye, such as spiropyran. Upon irradiation with ultraviolet (UV) light, the transparent spiropyran conformation will undergo a ring-opening transformation to the absorbing merocyanine form. The molecule can be reversibly switched back to its stable ring-closed configuration by exposure to heat or visible light. This strategy allows optical control over an active molecular plasmonic system by using light and/or heat to reversibly switch a molecular resonance. Pala et al. (42) used the photoisomerization property of spiropyran to create an all-optical plasmonic switch. Spiropyran molecules in a poly(methyl methacrylate) (PMMA) matrix were spin cast on an aluminum film containing gratings with different spacings. Surface plasmon polaritons were then launched in the aluminum film by coupling light into a grating, and the plasmon propagation lengths were measured as a function of the state of the spiropyran photochromic dye. When the molecules were in their absorbing merocyanine state, the plasmon polariton propagation length was significantly shortened compared to when the molecules were in their transparent spiropyran state. Using this geometry, the authors were able to reversibly turn the propagation of a plasmon on and off through optically induced changes in the interacting molecular layer. Weiss and coworkers (43) also exploited photochromism by doping spiropyran molecules into PMMA and spin casting the film onto an array of gold nanoparticles. By performing angle-resolved measurements, the authors were able to see the effects of both the change in the local refractive index and the change in the molecular resonance on the LSPR spectra of the nanoparticles. Bachelot and coworkers (44) performed a similar set of experiments on silver nanoparticle arrays and reported reversible changes in the LSPR spectra in which plasmon splitting was observed when the molecules were in the absorbing merocyanine form, but the original plasmon spectrum was restored when the molecules returned to the transparent spiropyran form.

As a third strategy, chemically controlling the electronic resonance of a molecule coupled to a plasmonic substrate also allows for direct tuning of the plasmon resonance. Wang and coworkers (45) prepared polyaniline/gold nanorod core/shell particles and demonstrated a reversible LSPR response upon changing the pH of the system, based on a change in the molecular resonance between the protonated and deprotonated forms of the polyaniline. Zheng et al. (8) used gold nanodisk arrays labeled with rotaxane molecules, which have two stable states with different electronic resonances. To switch between the states, chemical reducing and oxidizing agents were selectively allowed to interact with the rotaxane molecules. Similar to the results of Haes et al. (22) shown in **Figure 1**, Zheng et al. found that the magnitude of the LSPR shift response depended on the wavelength-dependent change in refractive index as the molecule was switched between oxidation states.

In the previous examples, the plasmonic properties of nanostructured metallic substrates were tuned by changing the electronic resonance of an adsorbed molecule. However, active molecular plasmonic devices can also be controlled by combining hybrid organic-plasmonic systems with traditional bulk refractive index sensitivity. For example, Odom and coworkers (46) built a tunable plasmonic laser in which a change in the bulk refractive index of the solvent environment yielded a distinct shift in the lasing wavelength. The laser is based on a gold nanoparticle array, which helps control the directionality of the emitted light, in contact with a solution containing the gain medium, infrared (IR)-40 dye molecules (shown schematically in **Figure 3a**). The solvent was changed from benzyl alcohol (BA) to dimethyl sulfoxide (DMSO), changing the refractive index environment and thus the plasmon resonance of the gold nanoparticle array (**Figure 3a**). This change in the local environment changed the lasing conditions of the device, allowing

PMMA: poly(methyl methacrylate)

BA: benzyl alcohol

DMSO: dimethyl sulfoxide

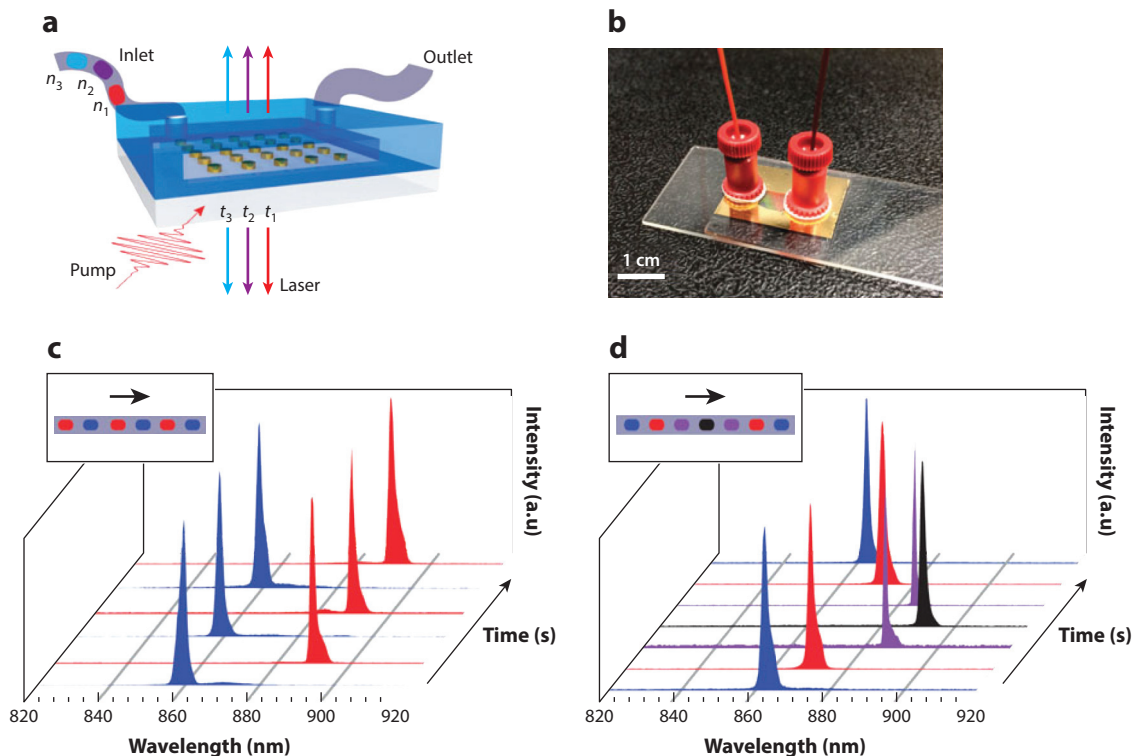


Figure 3

Active molecular plasmonic laser. (a) Schematic and (b) photograph of microfluidic device used to switch solvent refractive indices (shown in the schematic as colored “plugs” within the inlet line, with refractive indices n_1 – n_3) to tune the plasmon resonance of the gold nanoparticle array and lasing wavelength (colored arrows in the schematic). Dissolved infrared (IR)-40 molecules act as the gain medium. (c,d) Switching of the lasing wavelength as the solvent environment is changed from (c) dimethyl sulfoxide (DMSO; blue) to benzyl alcohol (BA; red) and (d) DMSO (blue), 2:1 DMSO:BA (red), 1:2 DMSO:BA (purple), and BA (black). Reprinted with permission from Reference 46. Copyright 2015 Nature Publishing Group.

the laser wavelength to be reversibly tuned as the solvent was changed from BA to DMSO (Figure 3c) or some mixture thereof (Figure 3d). Thus, the authors were able to attain active control of a plasmonic laser simply by exploiting the bulk refractive index sensitivity of the plasmonic component of the hybrid plasmon-molecule system.

MOLECULES AS HOT SPOTS: BEYOND THE ELECTROMAGNETIC APPROXIMATION IN SERS

In the previous section, the plasmon resonance was modulated dynamically by introducing molecules with tunable electronic resonances to plasmonic substrates. In those examples, the influence of the molecule was quite dramatic, leading to large changes in the plasmon resonance and extinction intensity. However, molecules can also play more subtle roles in interacting with plasmonic substrates, as is evident in recent SERS work. In SERS, the weak Raman scattering from a molecule is enhanced by many orders of magnitude when placed on or near a nanoscale-roughened metal surface. The dominant mechanism for SERS enhancement is the electromagnetic mechanism in which the excitation of a plasmon leads to a locally enhanced electromagnetic field

at the nanostructured surface (12). Because both the incident radiation and the Raman scattered light can interact with the plasmon, SERS is often referred to as an E^4 enhancement mechanism, where the SERS enhancement factor (EF) is given as:

$$\text{EF} = \left[\frac{E_{\text{loc}}(\omega_{\text{exc}})}{E_{\text{inc}}(\omega_{\text{exc}})} \right]^2 \left[\frac{E_{\text{loc}}(\omega_{\text{scat}})}{E_{\text{inc}}(\omega_{\text{scat}})} \right]^2 \quad 1.$$

EF: enhancement factor

Here, E_{loc} is the locally enhanced electromagnetic field, E_{inc} is the incident field, ω_{exc} is the frequency of the incident field, and ω_{scat} is the frequency of the Raman scattered light. Because ω_{exc} and ω_{scat} are often close in energy, Equation 1 is approximated as $\text{EF} \approx E^4$, where E represents the ratio of the enhanced field to the incident field.

Although this expression is a convenient representation of the SERS process, it ignores the role that the molecule plays in the SERS enhancement and, instead, assumes that plasmon-enhanced fields dominate both the excitation and emission properties. Thus, if plasmon excitation leads to an electromagnetic field enhancement of 100 at the nanoparticle surface, the SERS enhancement is predicted to be 10^8 . In the case of aggregated nanostructures, the enhanced electromagnetic fields in the junction region between adjacent nanoparticles can be sufficiently large to enable detection of a single molecule, leading to these regions being defined as hot spots (47–51). In the traditional picture, the emission from the single molecule is coupled out directly through the hot spot, meaning that all spatial information associated with the SERS emission from the molecule is dictated by the plasmonic nanostructure, and the molecule is just a passive observer (52).

Work from our group, however, showed that the molecule plays an active role in driving the SERS emission properties based on its position on the nanostructure surface (53–56). For our experiments, we prepared silver nanoparticle aggregates labeled with a single rhodamine 6G molecule, which serves as the SERS reporter. Because each individual aggregated nanostructure is smaller than the wavelength of light, the emission appears as a diffraction-limited spot when imaged onto a charge-coupled device camera (57). To find the approximate spatial origin of the emission, we fit the diffraction-limited single-molecule SERS emission to a two-dimensional Gaussian as shown:

$$I(x, y) = z_0 + I_0 e^{-\frac{1}{2} \left[\left(\frac{x - x_0}{s_x} \right)^2 + \left(\frac{y - y_0}{s_y} \right)^2 \right]} \quad 2.$$

Here, $I(x, y)$ is the intensity of the diffraction-limited emission on the camera, z_0 is the background intensity, I_0 is the peak emission intensity, x_0 and y_0 are the peak of the Gaussian, and s_x and s_y are the widths of the Gaussian in the x - and y -dimensions. If the SERS is radiated exclusively from the hot spot, we would expect to localize the centroid (e.g., x_0, y_0) to a single, stationary position associated with the junction region occupied by the molecule. Instead, we found that the calculated centroid position changed over time by tens of nanometers, suggesting a dynamic process that cannot be explained by the traditional model of stationary electromagnetic hot spot emission (53). Moreover, we saw that changes in the intensity of the SERS emission were related to the spatial origin of the signal, with a specific region in space associated with the strongest SERS intensity, accompanied by a gradient decay in the intensity as the emission centroid moved away from that spot. **Figure 4** shows two examples in which we use Equation 2 to calculate spatial intensity maps by plotting the average SERS intensity (represented by the color map) as a function of the spatial origin of the signal (x_0, y_0) (54). In both examples, we also show correlated scanning electron microscope images, and we find that the shape of the spatial intensity maps matches with structural features of the nanoparticle junctions. Importantly, we find that the SERS emission does not originate from a single position in space but instead changes in an intensity-dependent manner over the course of the experiment, suggesting that the emission does not originate exclusively from

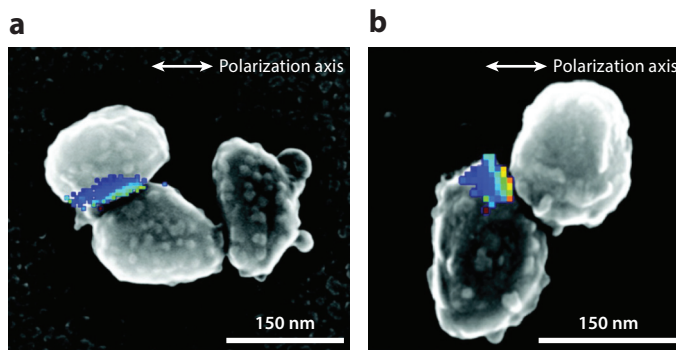


Figure 4

Examples correlating the spatial origin of different surface plasmon resonance emission intensities (*color map*) from single rhodamine 6G molecules with the structure of the underlying silver colloidal aggregates as determined by scanning electron microscopy. Adapted with permission from Reference 54. Copyright 2011 American Chemical Society.

the hot spot but rather is due to some coupling between the (mobile) molecule and the plasmon modes of the nanostructure.

To support this hypothesis, we turned to calculations from Ausman & Schatz (58) that show how the position of a molecule on the surface of a nanoparticle dimer can impact how light is radiated into the far field by the coupled system. When the molecule is directly in the junction between the two nanoparticles, light is radiated uniformly by the nanostructure, leading to a calculated centroid that would correspond to the position of the hot spot. However, when the molecule moves to a new position, it changes how the emission couples to the plasmon modes of the nanostructure, leading to emission that is biased toward the nanoparticle on which the molecule resides. As the molecule explores the nanoparticle surface, the expected centroid position shifts, as we observed experimentally, indicating that the molecule is not a passive observer in the SERS emission process but is instead an active participant in how and where light is radiated by the coupled molecule-plasmon system. Thus, the hot spot should be defined by the coupled molecule-plasmon emitter rather than the plasmon modes of the isolated nanostructure.

Jensen and coworkers (59) took this idea even further, and calculated SERS EFs in which they accounted for the role of the molecule. In their calculations, both the molecule and the nanoparticle were treated as polarizable objects that could interact with each other. This is a distinctly different view from the traditional picture in which the molecule is assumed to be too small to perturb the nanoparticle polarizability, leading to the treatment of SERS as a purely plasmon-driven electromagnetic effect based on the E^4 enhancement. **Figure 5** shows calculated SERS EFs using their discrete interaction model/quantum mechanics (DIM/QM) approach for a pyridine molecule interacting with a silver or gold nanoparticle. For comparison, the calculated EF using the E^4 approximation (Equation 1) is also included. Far from the nanoparticle surface, the DIM/QM and E^4 approaches show excellent agreement; however, as the molecule approaches the nanoparticle surface, significant differences between the two models emerge. In the case of the silver nanoparticle, the E^4 approximation overestimates the magnitude of the SERS enhancement as the molecule approaches the surface, whereas in the case of a gold nanoparticle, the DIM/QM method yields EFs that are actually higher than the E^4 mechanism would suggest. Furthermore, when a pyridine molecule and a gold nanoparticle are sufficiently close such that their electron distributions overlap, the electric field at the nanoparticle surface and the resultant enhancement factor decrease, as shown in **Figure 5b**.

DIM/QM: discrete interaction model/quantum mechanics

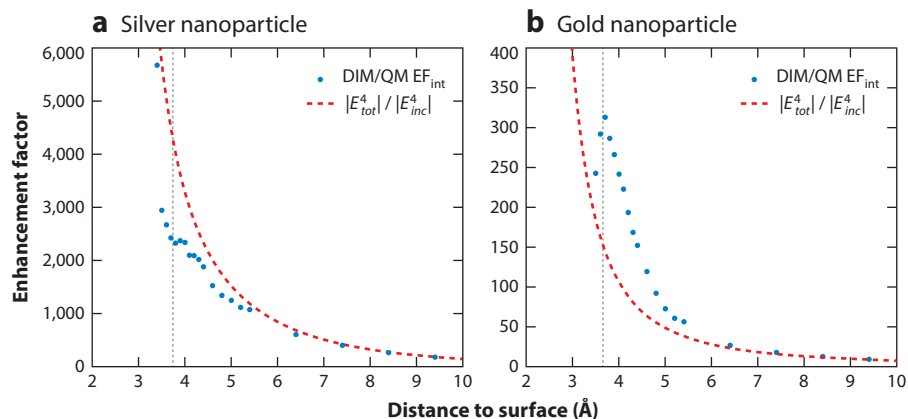


Figure 5

Enhancement factors (EFs) calculated using the E^4 method (red dotted line) and the discrete interaction model/quantum mechanics (DIM/QM) method (blue dots) for pyridine on (a) silver and (b) gold nanoparticles. EF differences between the methods occur when a molecule is near the nanoparticle surface, highlighting the importance of considering molecule-plasmon interactions. Reprinted with permission from Reference 59. Copyright 2014 American Chemical Society.

Both the experiments and calculations described above lead to a new paradigm for thinking about SERS: Instead of treating the SERS enhancement effect as originating from the nanoparticle alone, the role of the molecule must be included to generate a more complete picture of the coupled plasmon-molecule emitter. This is not a simple restatement of the chemical effect in SERS in which new hybrid charge transfer states can emerge when a molecule interacts with the metal (although these types of effects are also important when predicting SERS spectra and local EFs) (60, 61) but instead requires new models for thinking about how a molecule can impact the electromagnetic enhancement associated with a plasmon at a fundamental level. The LSPR work described in previous sections shows how overlap between molecular and plasmonic resonances can dramatically impact the spectral response of the plasmonic nanostructure, but the SERS work shows how interactions between polarizable species can have equally important roles in determining how molecular spectroscopies are impacted by plasmon-molecule coupling.

MOLECULES AS PLASMONIC MATERIALS

So far, all of the experiments described in this review have involved coupled molecular plasmonic systems in which the plasmonic material is a noble metal. One challenge with using metallic nanostructures as plasmonic substrates is the inherent particle-to-particle heterogeneity that exists due to the fact that we cannot control assembly at the atomic level. Both the number and arrangement of metal atoms will always vary even with the best synthetic or lithographic strategies. A second challenge is that the metals typically used in most plasmonic applications, gold and silver, are quite expensive and thus not useful for practical technologies that must be scalable for mass production.

In contrast to metallic nanostructures, molecules are defined by their chemical composition and atomic arrangement, allowing for excellent homogeneity and reproducibility of structure. Moreover, organic molecules are fairly inexpensive compared to noble metals, as is evident by the push

to move toward organic photovoltaics and other optoelectronic devices. Analogous to the surface conduction electrons that make up a plasmon in a metallic structure, conjugated molecules contain delocalized electrons in the π - π^* orbitals that allow the possibility of collective electron density displacement, making them strong candidates for supporting a molecular plasmon. Furthermore, a large library exists for the synthesis of a variety of conjugated molecules, which could allow for broad tunability if plasmons could be supported in such materials. Developing molecular plasmons would also allow a bottom-up approach to building plasmonic systems with nanometer precision.

Graphene has recently emerged as an intriguing two-dimensional material capable of supporting surface plasmon polaritons owing to its exceptional electrical properties, including a resistivity lower than that of noble metals (62). Graphene plasmons have already been demonstrated upon electrical doping (63, 64) and are tunable over a large spectral range by the level of charge doping (65). Decreasing the dimensionality of doped graphene sheets by cutting them into ribbons or folding them into nanotubes can shift the plasmon energy to biologically relevant near-IR wavelengths (66). Graphene plasmons have already been exploited for plasmon-based sensing (67), graphene-enhanced Raman scattering (68), and active plasmonic devices (69, 70), indicating the potential for organic plasmonic materials.

One challenge for plasmonic applications is that as graphene is cut into smaller constituent fused benzene rings, the semimetal band structure changes to resemble discrete molecules. Typically, this class of polycyclic aromatic hydrocarbons exhibits high energy band gaps with electronic transitions in the UV spectrum. Changing the charge state (by electron or hole injection) of the molecule can, however, change the electronic structure of these types of molecules so that new electronic transitions are available at lower energies, down into the visible spectrum (11, 71). In this situation, light may drive several individual, yet coherent, electron excitations that distribute the electrons and holes locally on the molecule. In acenes, for example, the HOMO (highest unoccupied molecular orbital)-1 \rightarrow LUMO (lowest unoccupied molecular orbital) and HOMO \rightarrow LUMO-1 excitations polarized along the longitudinal axis of the molecule add constructively, leading to electron density oscillating between the ends of the molecule (72). This asymmetric electron density distribution on the molecule sets up a dipolar resonance, as seen in traditional metal-based plasmonic materials. One key feature of the theoretically predicted plasmon modes is that the individual electron-hole transitions must be allowed to “see” each other in order to set up the collective electron motion associated with the traditional definition of a plasmon (73). If each electron-hole excitation is treated independently, with no interaction, then this theory does not converge to plasmon-like behavior, as shown by García de Abajo and coworkers (71).

Much like graphene, molecular plasmons in polycyclic aromatic hydrocarbons can be tuned through the degree of charge doping, down to the level of single-charge injection. García de Abajo and coworkers (71) predicted that by injecting an electron or hole in such a molecule, new absorption features would occur at visible frequencies. **Figure 6** shows an example from their work in which the plasmon resonance peak changes as the length of a polyacene molecule (**Figure 6a**) and number of injected charges varies (**Figure 6b**). No low-energy peaks are observed in the visible spectrum when the polyacene molecule is uncharged (no data shown), but when one or two charges are injected, a new low-energy plasmon mode appears at energies at or near the visible region of the electromagnetic spectrum. As the molecule length increases, the two modes shift to lower energy, similar to the red shift observed for longitudinal plasmon modes in nanorods with increasing aspect ratios (74). Moreover, as seen in the inset of **Figure 6b**, the induced charge distribution is highly dipolar along the long axis of the polyacene, further highlighting the similarity between the longitudinal mode of a nanorod and the dipolar plasmon in a linear polycyclic aromatic hydrocarbon molecule.

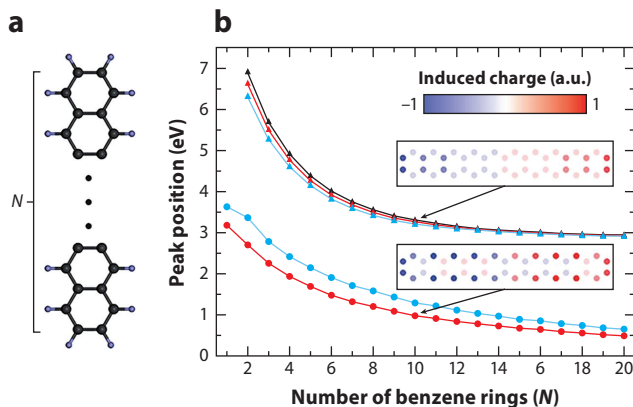


Figure 6

(a) Polyacene molecule with a varying number (N) of benzene units. (b) Lowest-energy (solid lines with circles) and second-lowest-energy (solid lines with triangles) plasmon modes, associated with zero charge (black), single charge (red), or double charge (light blue) injection. (Inset) Predicted charge distribution across a molecule with 10 fused benzene rings for the two lowest-energy modes with one injected electron. Adapted with permission from Reference 71. Copyright 2013 American Chemical Society.

Recently, plasmons in polycyclic aromatic hydrocarbons have been demonstrated experimentally by Halas and coworkers (11). In their experiment, several polycyclic aromatic hydrocarbons were electrochemically doped, resulting in changes in the color of the solution corresponding to newly created plasmon resonances in the visible spectrum. As with the theoretical calculations in **Figure 6**, an increase in the conjugation length of the molecule was experimentally found to red-shift the plasmon energy. Moreover, the molecular plasmons were found to be sensitive to the local refractive index, as evidenced by a red shift as the solvent refractive index increased. Thus, much of the existing intuition associated with traditional noble metal-based plasmonic materials seems to translate to molecular plasmons, offering a wide parameter space to explore these new and exciting materials.

CONCLUSIONS/OUTLOOK

In this review, we have discussed molecular plasmonics from a variety of perspectives: changes induced in plasmon resonance spectra associated with coupling to electronic resonances of molecules, active plasmonics driven by molecular-level control, SERS experiments and theory in which molecules impact the SERS emission properties, and even molecules as plasmonic materials. The general theme throughout each of these examples is simple: The molecule matters. It is this fundamental principle that distinguishes molecular plasmonics from plasmonics—namely, that the introduction of a molecule to a plasmonic substrate leads to measurable, and sometimes controllable, changes in the plasmonic properties of the material. Although this simple tenet has been exploited for a wide variety of plasmon-based sensing experiments (such as refractive index sensing and SERS), we have shown examples in which the molecule can have a larger than expected impact, by inducing large changes in plasmon resonance spectra (through dips, splitting, quenching, and shifts), impacting SERS emission beyond a simple plasmon-enhanced electromagnetic field picture, and even acting as the plasmonic substrate. Given the wide application space available for the use of coupling molecules and plasmonic materials, we expect this field to continue to expand, impacting sensing, optoelectronics, light-based nanocircuitry, and topics beyond.

DISCLOSURE STATEMENT

The authors are not aware of any affiliations, memberships, funding, or financial holdings that might be perceived as affecting the objectivity of this review.

ACKNOWLEDGMENTS

Work was supported by the US Department of Energy, Office of Science, and Basic Energy Sciences (DE-SC0010307).

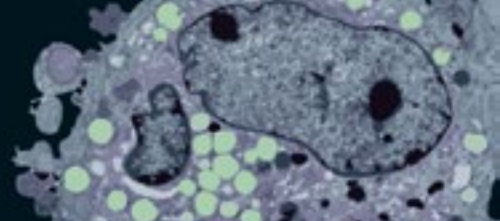
LITERATURE CITED

1. Sonntag MD, Klingsporn JM, Zrimsek AB, Sharma B, Ruvuna LK, Van Duyne RP. 2014. Molecular plasmonics for nanoscale spectroscopy. *Chem. Soc. Rev.* 43(4):1230–47
2. Zheng YB, Kiraly B, Weiss PS, Huang TJ. 2012. Molecular plasmonics for biology and nanomedicine. *Nanomedicine* 7(5):751–70
3. Csaki A, Schneider T, Wirth J, Jahr N, Steinbrück A, et al. 2011. Molecular plasmonics: Light meets molecules at the nanoscale. *Philos. Trans. R. Soc. A* 369(1950):3483–96
4. Prodan E, Radloff C, Halas NJ, Nordlander P. 2003. A hybridization model for the plasmon response of complex nanostructures. *Science* 302(5644):419–22
5. Nordlander P, Oubre C, Prodan E, Li K, Stockman MI. 2004. Plasmon hybridization in nanoparticle dimers. *Nano Lett.* 4(5):899–903
6. Prodan E, Nordlander P. 2004. Plasmon hybridization in spherical nanoparticles. *J. Chem. Phys.* 120(11):5444–54
7. Witlicki EH, Johnsen C, Hansen SW, Silverstein DW, Bottomley VJ, et al. 2011. Molecular logic gates using surface-enhanced Raman-scattered light. *J. Am. Chem. Soc.* 133(19):7288–91
8. Zheng YB, Yang Y-W, Jensen L, Fang L, Juluri BK, et al. 2009. Active molecular plasmonics: controlling plasmon resonances with molecular switches. *Nano Lett.* 9(2):819–25
9. Wurtz GA, Evans PR, Hendren W, Atkinson R, Dickson W, et al. 2007. Molecular plasmonics with tunable exciton–plasmon coupling strength in J-aggregate hybridized Au nanorod assemblies. *Nano Lett.* 7(5):1297–303
10. Van Duyne RP. 2004. Molecular plasmonics. *Science* 306(5698):985–86
11. Lauchner A, Schlather AE, Manjavacas A, Cui Y, McClain MJ, et al. 2015. Molecular plasmonics. *Nano Lett.* 15(9):6208–14
12. Willets KA, Van Duyne RP. 2007. Localized surface plasmon resonance spectroscopy and sensing. *Annu. Rev. Phys. Chem.* 58(1):267–97
13. Kelly KL, Coronado E, Zhao LL, Schatz GC. 2003. The optical properties of metal nanoparticles: the influence of size, shape, and dielectric environment. *J. Phys. Chem. B* 107(3):668–77
14. Haynes CL, Van Duyne RP. 2001. Nanosphere lithography: a versatile nanofabrication tool for studies of size-dependent nanoparticle optics. *J. Phys. Chem. B* 105(24):5599–611
15. Naik GV, Shalaev VM, Boltasseva A. 2013. Alternative plasmonic materials: beyond gold and silver. *Adv. Mater.* 25(24):3264–94
16. Lounis SD, Runnerstrom EL, Llordés A, Milliron DJ. 2014. Defect chemistry and plasmon physics of colloidal metal oxide nanocrystals. *J. Phys. Chem. Lett.* 5(9):1564–74
17. Homola J, Yee SS, Gauglitz G. 1999. Surface plasmon resonance sensors: review. *Sens. Actuators B* 54(1–2):3–15
18. Mock JJ, Smith DR, Schultz S. 2003. Local refractive index dependence of plasmon resonance spectra from individual nanoparticles. *Nano Lett.* 3(4):485–91
19. Anker JN, Hall WP, Lyandres O, Shah NC, Zhao J, Van Duyne RP. 2008. Biosensing with plasmonic nanosensors. *Nat. Mater.* 7(6):442–53

20. Moskovits M. 1985. Surface-enhanced spectroscopy. *Rev. Mod. Phys.* 57(3):783–826
21. Le Ru EC, Blackie E, Meyer M, Etchegoin PG. 2007. Surface enhanced Raman scattering enhancement factors: a comprehensive study. *J. Phys. Chem. C* 111(37):13794–803
22. Haes AJ, Zou S, Zhao J, Schatz GC, Van Duyne RP. 2006. Localized surface plasmon resonance spectroscopy near molecular resonances. *J. Am. Chem. Soc.* 128(33):10905–14
23. Kometani N, Tsunobuchi M, Fujita T, Asami K, Yonezawa Y. 2001. Preparation and optical absorption spectra of dye-coated Au, Ag, and Au/Ag colloidal nanoparticles in aqueous solutions and in alternate assemblies. *Langmuir* 17(3):578–80
24. Wiederrecht GP, Wurtz GA, Hranisavljevic J. 2004. Coherent coupling of molecular excitons to electronic polarizations of noble metal nanoparticles. *Nano Lett.* 4(11):2121–25
25. Fofang NT, Grady NK, Fan Z, Govorov AO, Halas NJ. 2011. Plexciton dynamics: exciton–plasmon coupling in a J-aggregate–Au nanoshell complex provides a mechanism for nonlinearity. *Nano Lett.* 11(4):1556–60
26. Zengin G, Wersäll M, Nilsson S, Antosiewicz TJ, Käll M, Shegai T. 2015. Realizing strong light-matter interactions between single-nanoparticle plasmons and molecular excitons at ambient conditions. *Phys. Rev. Lett.* 114(15):157401
27. Liu GL, Long Y-T, Choi Y, Kang T, Lee LP. 2007. Quantized plasmon quenching dips nanospectroscopy via plasmon resonance energy transfer. *Nat. Methods* 4(12):1015–17
28. Chen H, Shao L, Woo KC, Wang J, Lin H-Q. 2012. Plasmonic-molecular resonance coupling: plasmonic splitting versus energy transfer. *J. Phys. Chem. C* 116(26):14088–95
29. Zhao J, Das A, Schatz GC, Sligar SG, Van Duyne RP. 2008. Resonance localized surface plasmon spectroscopy: sensing substrate and inhibitor binding to cytochrome P450. *J. Phys. Chem. C* 112(34):13084–88
30. Wu L, Reinhard BM. 2014. Probing subdiffraction limit separations with plasmon coupling microscopy: concepts and applications. *Chem. Soc. Rev.* 43(11):3884–97
31. Lee SE, Chen Q, Bhat R, Petkiewicz S, Smith JM, et al. 2015. Reversible aptamer–Au plasmon rulers for secreted single molecules. *Nano Lett.* 15(7):4564–70
32. Huang F, Baumberg JJ. 2010. Actively tuned plasmons on elastomerically driven Au nanoparticle dimers. *Nano Lett.* 10(5):1787–92
33. Aksu S, Huang M, Artar A, Yanik AA, Selvarasah S, et al. 2011. Flexible plasmonics on unconventional and nonplanar substrates. *Adv. Mater.* 23(38):4422–30
34. Olcum S, Kocabas A, Ertas G, Atalar A, Aydinli A. 2009. Tunable surface plasmon resonance on an elastomeric substrate. *Opt. Express* 17(10):8542–47
35. Novo C, Funston AM, Gooding AK, Mulvaney P. 2009. Electrochemical charging of single gold nanorods. *J. Am. Chem. Soc.* 131(41):14664–66
36. Luther JM, Jain PK, Ewers T, Alivisatos AP. 2011. Localized surface plasmon resonances arising from free carriers in doped quantum dots. *Nat. Mater.* 10(5):361–66
37. Garcia G, Buonsanti R, Runnerstrom EL, Mendelsberg RJ, Llordes A, et al. 2011. Dynamically modulating the surface plasmon resonance of doped semiconductor nanocrystals. *Nano Lett.* 11(10):4415–20
38. Leroux YR, Lacroix JC, Chane-Ching KI, Fave C, Féridj N, et al. 2005. Conducting polymer electrochemical switching as an easy means for designing active plasmonic devices. *J. Am. Chem. Soc.* 127(46):16022–23
39. Leroux Y, Lacroix JC, Fave C, Trippe G, Féridj N, et al. 2008. Tunable electrochemical switch of the optical properties of metallic nanoparticles. *ACS Nano* 2(4):728–32
40. Leroux Y, Lacroix JC, Fave C, Stockhausen V, Féridj N, et al. 2009. Active plasmonic devices with anisotropic optical response: a step toward active polarizer. *Nano Lett.* 9(5):2144–48
41. Deleted in proof
42. Pala RA, Shimizu KT, Melosh NA, Brongersma ML. 2008. A nonvolatile plasmonic switch employing photochromic molecules. *Nano Lett.* 8(5):1506–10
43. Zheng YB, Kiraly B, Cheunkar S, Huang TJ, Weiss PS. 2011. Incident-angle-modulated molecular plasmonic switches: a case of weak exciton–plasmon coupling. *Nano Lett.* 11(5):2061–65
44. Baudrion A-L, Perron A, Veltri A, Bouhelier A, Adam P-M, Bachelot R. 2013. Reversible strong coupling in silver nanoparticle arrays using photochromic molecules. *Nano Lett.* 13(1):282–86

45. Jiang N, Shao L, Wang J. 2014. (Gold nanorod core)/(polyaniline shell) plasmonic switches with large plasmon shifts and modulation depths. *Adv. Mater.* 26(20):3282–89
46. Yang A, Hoang TB, Dridi M, Deeb C, Mikkelsen MH, et al. 2015. Real-time tunable lasing from plasmonic nanocavity arrays. *Nat. Commun.* 6:6939
47. Hao E, Schatz GC. 2004. Electromagnetic fields around silver nanoparticles and dimers. *J. Chem. Phys.* 120(1):357–66
48. Camden JP, Dieringer JA, Wang Y, Masiello DJ, Marks LD, et al. 2008. Probing the structure of single-molecule surface-enhanced Raman scattering hot spots. *J. Am. Chem. Soc.* 130(38):12616–17
49. Nie S, Emory SR. 1997. Probing single molecules and single nanoparticles by surface-enhanced Raman scattering. *Science* 275(5303):1102–6
50. Kneipp K, Wang Y, Kneipp H, Perelman LT, Itzkan I, et al. 1997. Single molecule detection using surface-enhanced Raman scattering (SERS). *Phys. Rev. Lett.* 78(9):1667–70
51. Le Ru EC, Etchegoin PG. 2012. Single-molecule surface-enhanced Raman spectroscopy. *Annu. Rev. Phys. Chem.* 63(1):65–87
52. Stockman M. 2006. Electromagnetic theory of SERS. In *Surface-Enhanced Raman Scattering*, ed. K Kneipp, M Moskovits, H Kneipp, pp. 47–65. Berlin: Springer
53. Stranahan SM, Willets KA. 2010. Super-resolution optical imaging of single-molecule SERS hot spots. *Nano Lett.* 10(9):3777–84
54. Weber ML, Willets KA. 2011. Correlated super-resolution optical and structural studies of surface-enhanced Raman scattering hot spots in silver colloid aggregates. *J. Phys. Chem. Lett.* 2(14):1766–70
55. Weber ML, Litz JP, Masiello DJ, Willets KA. 2012. Super-resolution imaging reveals a difference between SERS and luminescence centroids. *ACS Nano* 6(2):1839–48
56. Titus EJ, Weber ML, Stranahan SM, Willets KA. 2012. Super-resolution SERS imaging beyond the single-molecule limit: an isotope-edited approach. *Nano Lett.* 12(10):5103–10
57. Willets KA. 2014. Super-resolution imaging of SERS hot spots. *Chem. Soc. Rev.* 43(11):3854–64
58. Ausman LK, Schatz GC. 2009. On the importance of incorporating dipole reradiation in the modeling of surface enhanced Raman scattering from spheres. *J. Chem. Phys.* 131(8):084708
59. Payton JL, Morton SM, Moore JE, Jensen L. 2014. A hybrid atomistic electrodynamics-quantum mechanical approach for simulating surface-enhanced Raman scattering. *Acc. Chem. Res.* 47(1):88–99
60. Lombardi JR, Birke RL, Lu T, Xu J. 1986. Charge-transfer theory of surface enhanced Raman spectroscopy: Herzberg–Teller contributions. *J. Chem. Phys.* 84(8):4174–80
61. Morton SM, Jensen L. 2009. Understanding the molecule—surface chemical coupling in SERS. *J. Am. Chem. Soc.* 131(11):4090–98
62. Castro Neto AH, Guinea F, Peres NMR, Novoselov KS, Geim AK. 2009. The electronic properties of graphene. *Rev. Mod. Phys.* 81(1):109–62
63. Ju L, Geng B, Horng J, Girit C, Martin M, et al. 2011. Graphene plasmonics for tunable terahertz metamaterials. *Nat. Nano* 6(10):630–34
64. Koppens FHL, Chang DE, García de Abajo FJ. 2011. Graphene plasmonics: a platform for strong light-matter interactions. *Nano Lett.* 11(8):3370–77
65. Politano A, Chiarello G. 2014. Plasmon modes in graphene: status and prospect. *Nanoscale* 6(19):10927–40
66. García de Abajo FJ. 2014. Graphene plasmonics: challenges and opportunities. *ACS Photonics* 1(3):135–52
67. Marini A, Silveiro I, García de Abajo FJ. 2015. Molecular sensing with tunable graphene plasmons. *ACS Photonics* 2(7):876–82
68. Ling X, Huang S, Deng S, Mao N, Kong J, et al. 2015. Lighting up the Raman signal of molecules in the vicinity of graphene related materials. *Acc. Chem. Res.* 48(7):1862–70
69. Bao Y, Zu S, Zhang Y, Fang Z. 2015. Active control of graphene-based unidirectional surface plasmon launcher. *ACS Photonics* 2(8):1135–40
70. Manjavacas A, Thongrattanasiri S, Greffet J-J, García de Abajo FJ. 2014. Graphene optical-to-thermal converter. *Appl. Phys. Lett.* 105(21):211102

71. Manjavacas A, Marchesin F, Thongrattanasiri S, Koval P, Nordlander P, et al. 2013. Tunable molecular plasmons in polycyclic aromatic hydrocarbons. *ACS Nano* 7(4):3635–43
72. Guidez EB, Aikens CM. 2013. Origin and TDDFT benchmarking of the plasmon resonance in acenes. *J. Phys. Chem. C* 117(41):21466–75
73. Bernadotte S, Evers F, Jacob CR. 2013. Plasmons in molecules. *J. Phys. Chem. C* 117(4):1863–78
74. Link S, El-Sayed MA. 1999. Spectral properties and relaxation dynamics of surface plasmon electronic oscillations in gold and silver nanodots and nanorods. *J. Phys. Chem. B* 103(40):8410–26



New From Annual Reviews:

Annual Review of Cancer Biology

cancerbio.annualreviews.org • Volume 1 • March 2017

ONLINE NOW!

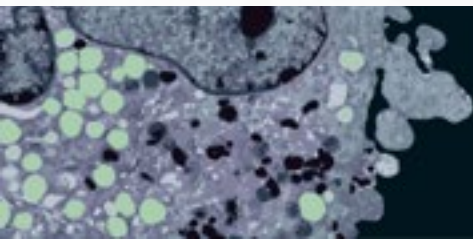
Co-Editors: **Tyler Jacks**, *Massachusetts Institute of Technology*

Charles L. Sawyers, *Memorial Sloan Kettering Cancer Center*

The *Annual Review of Cancer Biology* reviews a range of subjects representing important and emerging areas in the field of cancer research. The *Annual Review of Cancer Biology* includes three broad themes: Cancer Cell Biology, Tumorigenesis and Cancer Progression, and Translational Cancer Science.

TABLE OF CONTENTS FOR VOLUME 1:

- *How Tumor Virology Evolved into Cancer Biology and Transformed Oncology*, Harold Varmus 
- *The Role of Autophagy in Cancer*, Naiara Santana-Codina, Joseph D. Mancias, Alec C. Kimmelman
- *Cell Cycle–Targeted Cancer Therapies*, Charles J. Sherr, Jiri Bartek
- *Ubiquitin in Cell-Cycle Regulation and Dysregulation in Cancer*, Natalie A. Borg, Vishva M. Dixit
- *The Two Faces of Reactive Oxygen Species in Cancer*, Colleen R. Reczek, Navdeep S. Chandel
- *Analyzing Tumor Metabolism In Vivo*, Brandon Faubert, Ralph J. DeBerardinis
- *Stress-Induced Mutagenesis: Implications in Cancer and Drug Resistance*, Devon M. Fitzgerald, P.J. Hastings, Susan M. Rosenberg
- *Synthetic Lethality in Cancer Therapeutics*, Roderick L. Beijersbergen, Lodewyk F.A. Wessels, René Bernards
- *Noncoding RNAs in Cancer Development*, Chao-Po Lin, Lin He
- *p53: Multiple Facets of a Rubik's Cube*, Yun Zhang, Guillermina Lozano
- *Resisting Resistance*, Ivana Bozic, Martin A. Nowak
- *Deciphering Genetic Intratumor Heterogeneity and Its Impact on Cancer Evolution*, Rachel Rosenthal, Nicholas McGranahan, Javier Herrero, Charles Swanton
- *Immune-Suppressing Cellular Elements of the Tumor Microenvironment*, Douglas T. Fearon
- *Overcoming On-Target Resistance to Tyrosine Kinase Inhibitors in Lung Cancer*, Ibiayi Dagogo-Jack, Jeffrey A. Engelman, Alice T. Shaw
- *Apoptosis and Cancer*, Anthony Letai
- *Chemical Carcinogenesis Models of Cancer: Back to the Future*, Melissa Q. McCreery, Allan Balmain
- *Extracellular Matrix Remodeling and Stiffening Modulate Tumor Phenotype and Treatment Response*, Jennifer L. Leight, Allison P. Drain, Valerie M. Weaver
- *Aneuploidy in Cancer: Seq-ing Answers to Old Questions*, Kristin A. Knouse, Teresa Davoli, Stephen J. Elledge, Angelika Amon
- *The Role of Chromatin-Associated Proteins in Cancer*, Kristian Helin, Saverio Minucci
- *Targeted Differentiation Therapy with Mutant IDH Inhibitors: Early Experiences and Parallels with Other Differentiation Agents*, Eytan Stein, Katharine Yen
- *Determinants of Organotropic Metastasis*, Heath A. Smith, Yibin Kang
- *Multiple Roles for the MLL/COMPASS Family in the Epigenetic Regulation of Gene Expression and in Cancer*, Joshua J. Meeks, Ali Shilatifard
- *Chimeric Antigen Receptors: A Paradigm Shift in Immunotherapy*, Michel Sadelain





Contents

Applications of Optical Microcavity Resonators in Analytical Chemistry <i>James H. Wade and Ryan C. Bailey</i>	1
Molecular Plasmonics <i>Andrew J. Wilson and Katherine A. Willets</i>	27
Advances in Mid-Infrared Spectroscopy for Chemical Analysis <i>Julian Haas and Boris Mizaikoff</i>	45
In Situ and In Vivo Molecular Analysis by Coherent Raman Scattering Microscopy <i>Chien-Sheng Liao and Ji-Xin Cheng</i>	69
Advances in Magnetic Resonance Imaging Contrast Agents for Biomarker Detection <i>Sanbita Sinharay and Mark D. Pagel</i>	95
Progress in the Analysis of Complex Atmospheric Particles <i>Alexander Laskin, Mary K. Gilles, Daniel A. Knopf, Bingbing Wang, and Swarup China</i>	117
Electroanalytical Ventures at Nanoscale Interfaces Between Immiscible Liquids <i>Damien W.M. Arrigan and Yang Liu</i>	145
Reagentless, Structure-Switching, Electrochemical Aptamer-Based Sensors <i>Lauren R. Schoukroun-Barnes, Florika C. Macazo, Brenda Gutierrez, Justine Lottermoser, Juan Liu, and Ryan J. White</i>	163
New Functionalities for Paper-Based Sensors Lead to Simplified User Operation, Lower Limits of Detection, and New Applications <i>Josephine C. Cunningham, Paul R. DeGregory, and Richard M. Crooks</i>	183
Fabrication and Operation of Paper-Based Analytical Devices <i>Xiao Jiang and Z. Hugh Fan</i>	203

Glycan Arrays: From Basic Biochemical Research to Bioanalytical and Biomedical Applications <i>Andreas Geissner and Peter H. Seeberger</i>	223
Microfluidic Devices for the Measurement of Cellular Secretion <i>Adrian M. Schrell, Nikita Mukhitov, Lian Yi, Xue Wang, and Michael G. Roper</i>	249
Plant Molecular Farming: Much More than Medicines <i>Marc Tschofen, Dietmar Knopp, Elizabeth Hood, and Eva Stöger</i>	271
Methods for the Analysis of Protein Phosphorylation–Mediated Cellular Signaling Networks <i>Forest M. White and Alejandro Wolf-Yadlin</i>	295
Recent Progress in Monolithic Silica Columns for High-Speed and High-Selectivity Separations <i>Tobru Ikegami and Nobuo Tanaka</i>	317
Mass-Selective Chiral Analysis <i>Ulrich Boesl and Aras Kartouzian</i>	343
The Coupled Chemical and Physical Dynamics Model of MALDI <i>Richard Knochenmuss</i>	365
Advanced Multidimensional Separations in Mass Spectrometry: Navigating the Big Data Deluge <i>Jody C. May and John A. McLean</i>	387
Development and Applications of Liquid Sample Desorption Electrospray Ionization Mass Spectrometry <i>Qiuling Zheng and Hao Chen</i>	411
Mass Spectrometry Applied to Bottom-Up Proteomics: Entering the High-Throughput Era for Hypothesis Testing <i>Ludovic C. Gillet, Alexander Leitner, and Ruedi Aebersold</i>	449
Mass Spectrometry as a Preparative Tool for the Surface Science of Large Molecules <i>Stephan Rauschenbach, Markus Ternes, Ludger Harnau, and Klaus Kern</i>	473
Progress in Top-Down Proteomics and the Analysis of Proteoforms <i>Timothy K. Toby, Luca Fornelli, and Neil L. Kelleher</i>	499
Proteogenomics: Integrating Next-Generation Sequencing and Mass Spectrometry to Characterize Human Proteomic Variation <i>Gloria M. Sheynkman, Michael R. Shortreed, Anthony J. Cesnik, and Lloyd M. Smith</i>	521